Monitoring Elbow Isometric Contraction by Novel Wearable Fabric Sensing Device

Xi Wang[1], Xiaoming Tao[1,2]*, Raymond C.H. So[3] , Lin Shu[1], Bao Yang[1] and Ying Li[1]

[1]Institute of Textiles and Clothing

[2]Multidisciplinary Division of Bioengineering

The Hong Kong Polytechnic University

[3]Hong Kong Sports Institute

Hong Kong, China

*Corresponding author: Xiaoming Tao; Institute of Textiles and Clothing, The Hong Kong Polytechnic University, Kowloon, Hong Kong; 852-27666470;

Email: xiao-ming.tao@polyu.edu.hk

The following publication Wang, X., Tao, X., So, R. C., Shu, L., Yang, B., & Li, Y. (2016). Monitoring elbow isometric contraction by novel wearable fabric sensing device. Smart Materials and Structures, 25(12), 125022 is available at https://doi.org/10.1088/0964-1726/25/12/125022.

Abstract:

Fabric-based wearable technology is much desirable in sport, as it is light, flexible, soft, and comfortable with little interfere to normal sport activities. It can provide accurate information on in-situ deformation of muscles in a continuous and wireless manner. During elbow flexion in isometric contraction, upper arm circumference increases with contraction of elbow flexors, it is possible to monitor muscles' contraction by limb circumferential strains. This paper presents a new wireless wearable anthropometric monitoring device made from fabric strain sensors for human upper arm. The materials, structural design and calibration of the device are presented. Using isokinetic testing system (Biodex3®) and the fabric monitoring device simultaneously, in-situ measurements were carried out on elbow flexors in isometric contraction mode with 10 subjects for a set of positions. Correlations between the measured values of limb circumferential strain and normalized torque were examined, and a linear relationship was found during isometric contraction. The average correlation coefficient between them is 0.938±0.050. This wearable anthropometric device thus provides a useful index, the limb circumferential strain, for upper arm muscle contraction in isometric mode.

Keywords: Muscle deformation, limb circumferential strain (LCS), normalized torque (NT), fabric strain sensor

1. **Introduction**

As the motor of the human musculoskeletal system, skeletal muscles have been attracting great attentions of sportsmen, coaches and researchers [1-3]. For example, in the training of barbell curl for weightlifters, the real-time contractile properties of elbow flexors, especially intensity and efficiency of biceps brachii, are of the most interest to boost training results [4, 5] and assist rehabilitation. Therefore, over the past decades, efforts have been made to monitor muscle contraction continuously with noninvasive approaches [6-12], to correlate bioelectricity of superficial skeletal muscles (surface electromyography [6, 7, 13-16]), low-frequency oscillation of firing muscle fibers (mechanomyography [12, 16, 17]), as well as changing in morphology parameters of muscles during contraction (ultrasound [8-11, 18]),with muscular contraction status.

Due to the inherent defect of susceptible to environmental noises, surface electromyography (sEMG) was observed with under- or over- estimation occasionally in indexing the muscle contraction [15]. The mechanomyography (MMG) has been facing similar dilemma, only in the low-frequency band [17, 19]. In contrast, the ultrasound technology has been applied in detecting morphological deformation of skeletal muscles in real-time, which is more direct and stable. Through image processing of cross-sectional area of skeletal muscles, the morphological parameters, such as the changes in cross-section area [8, 9, 18, 20] and muscle volume[10, 11], muscle thickness and fiber pennation[7, 16, 21] of skeletal muscle have all been reported as index of contractile force during contraction, and correlations between the morphological parameters and generated joint torque were achieved[7, 16, 22, 23]. The

ultrasound method, relying on image processing technologies, induces errors caused by environmental noises. Moreover, the reported devices were expensive, not portable thus only limited to laboratory use, not applicable in the sport field.

During muscle contraction, myoin filaments and actin filaments in the muscle fiber embraces each other, leading to the shortening in length and enlargement in cross-sectional area. For parallel-fibered muscles such as biceps brachii, the accumulated thickening in activated muscle fibers directly causes the whole muscle to expand in cross-sectional area [24, 25]. This provides possibility of indexing muscle contraction status with real-time anthropometric parameters such as circumferences of some limbs (upper arm), whose contractors (biceps) dominate the increment of circumference during contraction. This would be a direct, portable and convenient method if successful [26-28]. For in-situ measurement, a flexible device is required to be worn on the curved and soft human skins in motion.

Recent years have seen arising and improvement of the wearable monitoring technologies [29-33]. Among those published works on anthropometric measurement, a wearable muscle circumferential sensor was developed to predict contractile force of biceps brachii during isotonic contraction based on a modified Hill's model [34]. However, the device was made of rigid metal wire, not soft enough. The circumference-to-torque model replaced electromyography with the relative changing rate of circumference of the upper arm as muscle activation level, which was a bold attempt that requires strong justifications. The error between the predicted torque and the measured torque during elbow isotonic contraction was

as large as 38%. This was attributed to the lack of fundamental study on the relationship between muscles' contraction and limb circumferential strain.

To explore the basic biomechanics and to better explore the relationship between skeletal muscle's contraction and limb circumferential strain, this paper describes a novel approach to monitor muscle deformation using a newly developed wireless limb gauge measurement system (LGMS) based on fabric sensing technology. The fabric sensors are flexible and ideal to seamlessly contact human skins, stretchable repeatedly with a large deformation up to 60% strain, durable with a fatigue life of 100,000 cycles as well as reliable with a measurement error of <5% and small hysteresis of ±3.5%. Equally importantly, the fabric-based system can continuously measure limb circumferential strain (LCS) in real time without any discomfort, which makes it wearable and superior in portability and convenience in sports monitoring systems. As the very initial part of the study of muscles' deformation during elbow movements such as barbell curl, which is indicated by the LCS, this paper mainly focus on the sensing mechanism and basic sensing behavior of the LGMS in elbow isometric contraction. The observed results establish and consolidate the relationship between muscle contractile force and the acquired anthropometric parameter, LCS, obtained from the fabric sensors.

2. Structural Design, Materials, fabrication and Calibration of the LGMS

2.1. Hypothesis and structural design

Previously, various parameters have been used for muscle contraction abilities and contractile force. Static cross sectional area has been used as an index for muscle contraction abilities [23], while other continuous anthropometric measures, such as muscle thickness and limb's circumferences can reflect the contraction states of skeletal muscles in motion, since skeletal muscles' contractions are always accompanied by their morphological changes. Investigations on upper extremities or lower extremities through ultrasound detection have proposed relationships between muscle thickness and torque, which is the representation of the contractile force [7, 16, 23]. Several published papers correlated limb circumference with torque [26, 28, 34] without elaborating its underlying mechanism.

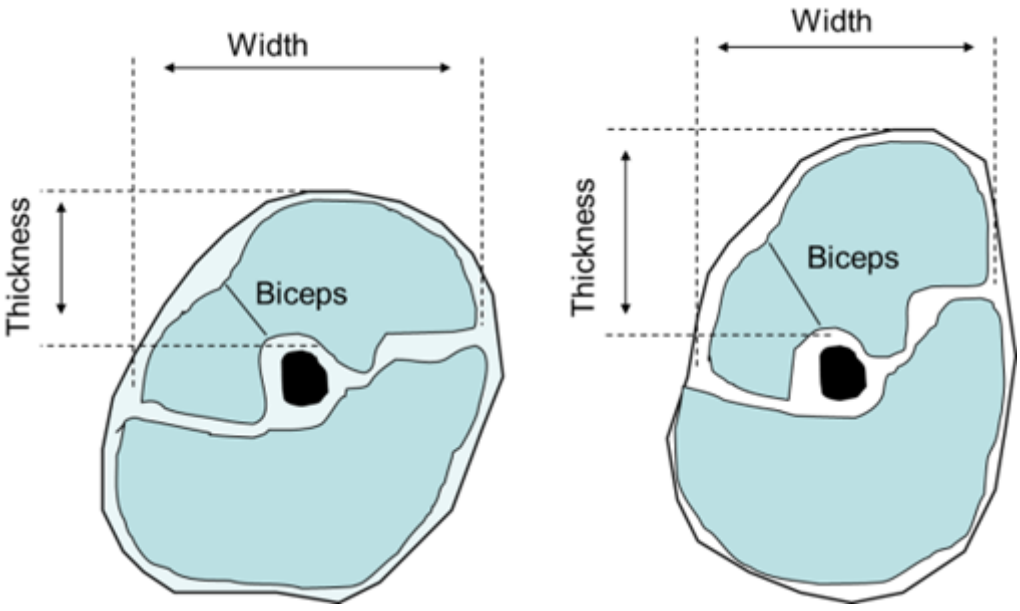

(a)

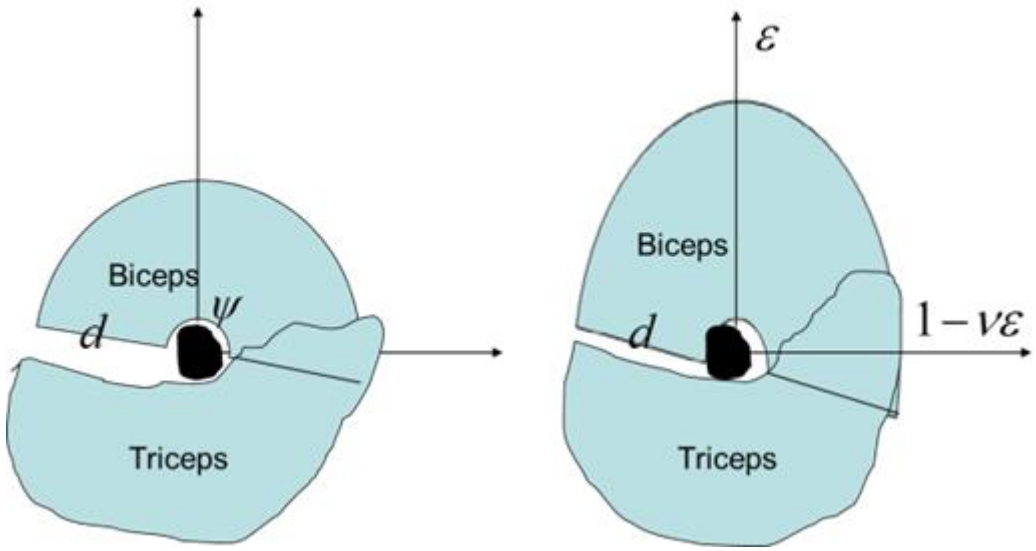

(b)

Figure 1 (a) Cross-section view of human upper arm, with biceps relaxed (left) and contracted (right), (b) Simplified model of the morphological change due to biceps contraction: relaxed (left); contracted (right)

Figure 1(a) and (b) illustrate the schematic and geometric interpretation, respectively, of how LCS represents the contraction levels. Figure 1(a) shows the cross section of human upper arm in relaxation and in 33% maximum voluntary flexion, respectively. The two sectors in Figure 1(b) depict biceps and the other tissues.

Accordingly, the muscle thickness can be an index for muscle contraction, while muscle volume seldom changes during contraction [35]. Hence, one can reasonably assume that the reduction in width is caused by the lengthening in the thickness, i.e.,

$$
\begin{aligned}
C_0 &= \psi \cdot d + C_t \\
C_1 &= \psi \cdot d \cdot \frac{\left(2 + \varepsilon - \nu \cdot \varepsilon\right)}{2} + C_t \\
\frac{\Delta C}{C_0} &= \frac{C_1 - C_0}{C_0} = \varepsilon \cdot \frac{1-\nu}{2} \cdot \psi \cdot \frac{d}{C_0} \\
LCS &= \frac{\Delta C}{C_0}
\end{aligned}
\tag{1}
$$

where C_0 is the upper arm circumference of the cross section in relaxation, C_1 is the circumference of cross section in contraction, C_t is the circumference of the other un-deforming sector (representing triceps and brachialis, whose morphologies are considered unchanged during contraction), ψ is the angle of the deforming sector and is approximately equal to π, d is the radius of the cross section in relaxation and is also the initial thickness, ε is the strain along the thickness direction, and ν is Poisson ratio of the muscle. Based on the assumptions, a linear relationship can be derived between ε (strain in thickness direction) and LCS, indicating that circumference of human upper arm may serve as an index of deformation of biceps during contraction, which is in accordance with previous works [26].

2.2. System structure

A flexible and soft limb gauge measurement system, as shown in Figure 2(a)), was designed, fabricated and characterized. The system can continuously measure the circumferences of limbs in motion and wirelessly sending the real-time signals to PCs or smart mobile phones via low-power Bluetooth. The system consists of three parts, i.e., fabric sensing belt, data acquisition/transmission module (DAQ), and user interface on a PC (Figure 2(b)).

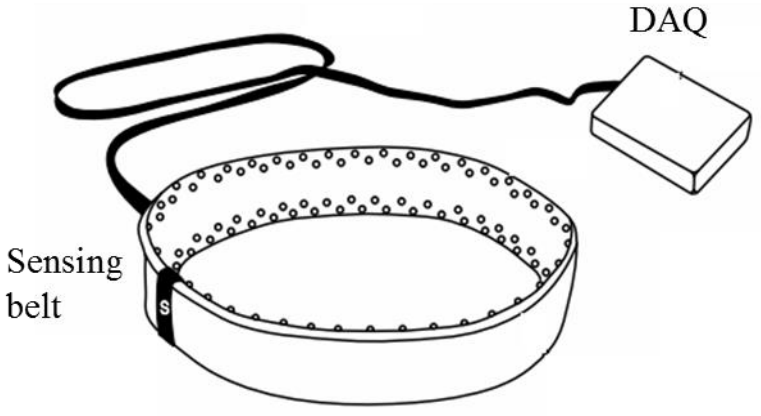

(a)

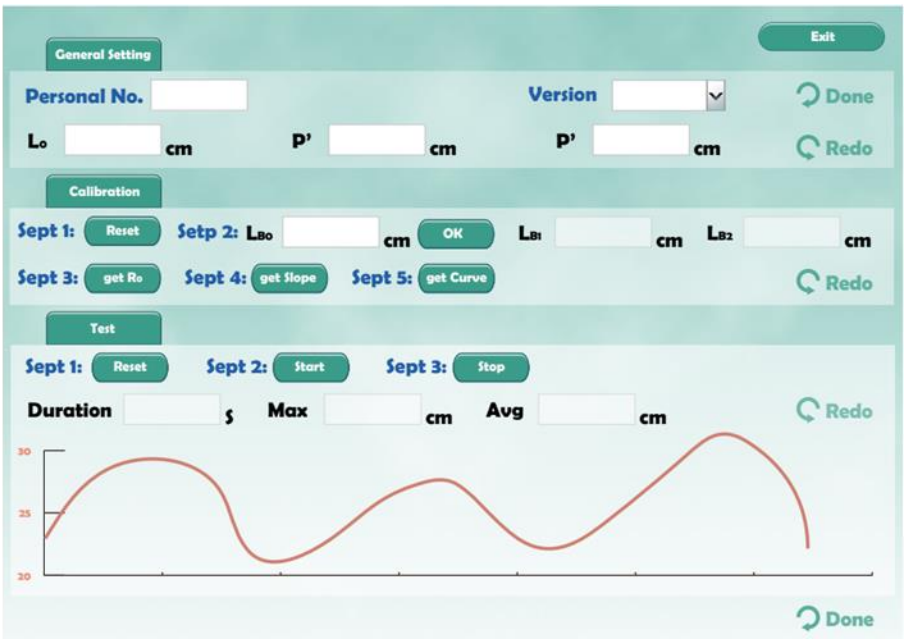

(b)

Figure 2 (a) Structure of sensing belt, DAQ and sensing belt of LMS with fabric strain sensor inside, (b) User Interface of the LMS

2.3. Fabric strain sensors and the sensing belt

The belt is composed of several sensing elements in an array, i.e., fabric strain sensors (FSSs) (Figure 3(a)), which were obtained from Advanpro Limited, Hong Kong. Fabricated by printing carbon nano-composites on a knitted fabric, the FSSs have been successfully applied in the field of smart textiles, including the pressures sensors for impact sensing[36], smart

shoes [37-39] to detect and prevent possible damages of the diabetics and the smart belt for monitoring the heart rate and respiratory rate in real-time [38, 39].

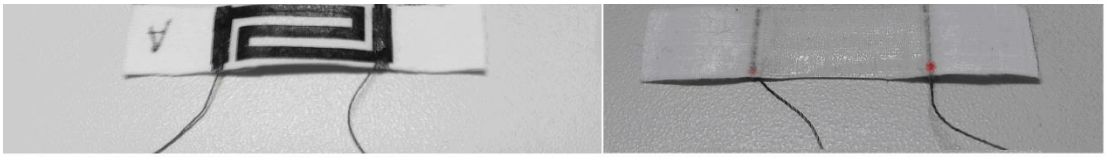

(a)

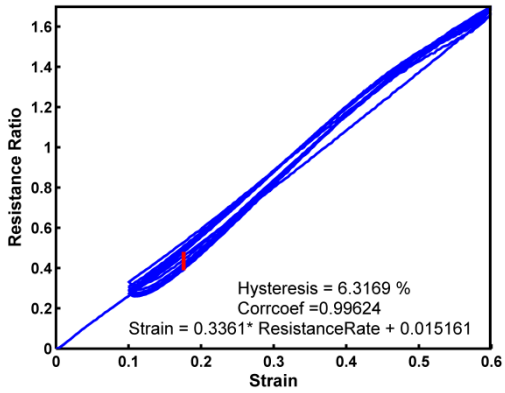

(b)

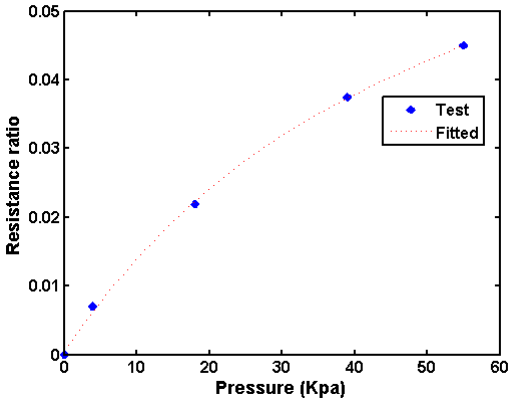

(c)

Figure 3 (a) The fabric strain sensor, front (left) and back (right), sensing area 8mm*25mm, (b) Mechanical-electrical properties of the FSS, (c) Effect of out-plane pressure on the resistance rate of FSS

The FSSs are soft, flexible, stretchable for a large deformation and capable of serving under a fatigue limit of about 100,000 cycles for a fairly broad working range of 60%. These merits

make FSSs feasible and suitable for human daily-wear equipment such as shoes, shirts and belts. The strain gauge factor of the FSS can be adjusted according to application requirements [38]. The measuring error of FSS was controlled within 5% and hysteresis was as low as ±3.5%. In the present study, the s-shape FSS (Figure 3(a)) was selected for its stable mechanical-electrical performance (table 1). Silicone elastomers were coated on both sides of the s-shape FSSs to prevent moisture and other disturbance from the environment.

Table 1 Performance specifications of fabric sensor elements

Performance	**Sensor element**
Strain measurement range	0-60%
Linearity	±5%
Repeatability	±5%
Hysteresis	±5%
Gauge factor	1-100
Working temperature	0-60℃
Fatigue resistance	>100,000 cycles
Temperature compensation range	0-60℃
Relaxation	±5%/30min
Zero-drift with time	±5%/h

Figure 3(b) illustrates a representative 10-cycle loading-unloading calibration curve of strain-resistance rate of the FSS (on INSTRON™ 5944), which shows a good linearity of 0.996, low hysteresis of ±3.16%, low stiffness of 1.16N, and good repeatability. In addition, the effect of the out-plane pressure on FSS was also studied, and with a measuring error not higher than 0.1% (Figure 3(c)) and thus being negligible up to 60kPa.

In order to detect in-position strain around human limb (human upper arm in this study), multiple FSSs were assembled with a 5% pre-tension on an elastic carrier made of fabric belt,

which was selected for good elasticity and good resilience (table 2). The FSSs and the carrier were protected by a covering package. Antiskid granules stuck on the inner side and on the covering package prevent sliding between skin and the belt, ensuring that local strains measured by the FSSs are in-position (Figure 4). Enameled copper wire in a zigzag pattern was used to electrically and physically connect the n FSSs to outer circuits in a '$n+1$' array, in which one electrical wire was adopted as ground line.

Table 2 Mechanical properties of the carrier (Standard: BS EN 14704, Specimens were held for 15 min)

Dimensions (width*length*thickness)	Unrecovered extension (mm)	Modulus/N (0%~60% elongation)	Ratio of Force Decay (%)
20mm*100mm*1mm	6.56	12.62	11.43

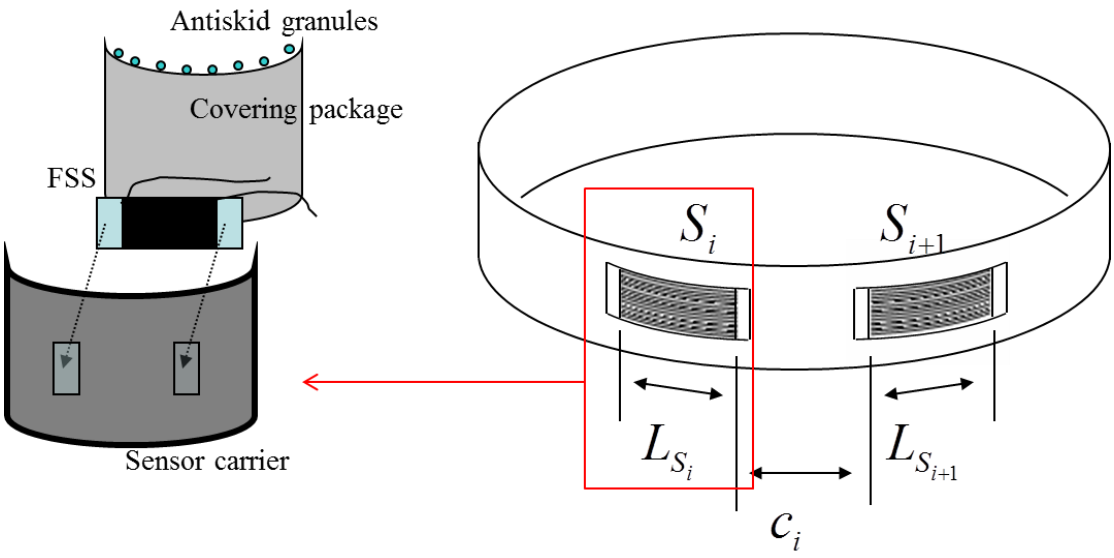

Figure 4 Structure of the sensing belt

To obtain an evaluation of the circumferential change of the belt, dimensions of the FSSs and in-position strains measured by the individual FSSs were required to calculate the circumference of upper arm and its change ratio (LCS). Therefore, FSSs were uniformly distributed around the carrier, except for the beginning and ending parts, which were occupied for wires' connection and calibration procession. A preliminary test in the cyclic flexions and extensions of elbow verified that strains measured by the FSSs were in exactly similar trends regardless of the position of the FSSs, owing to the fact that biceps brachii dominates circumferential strain of the upper arms in motion (Figure 5).

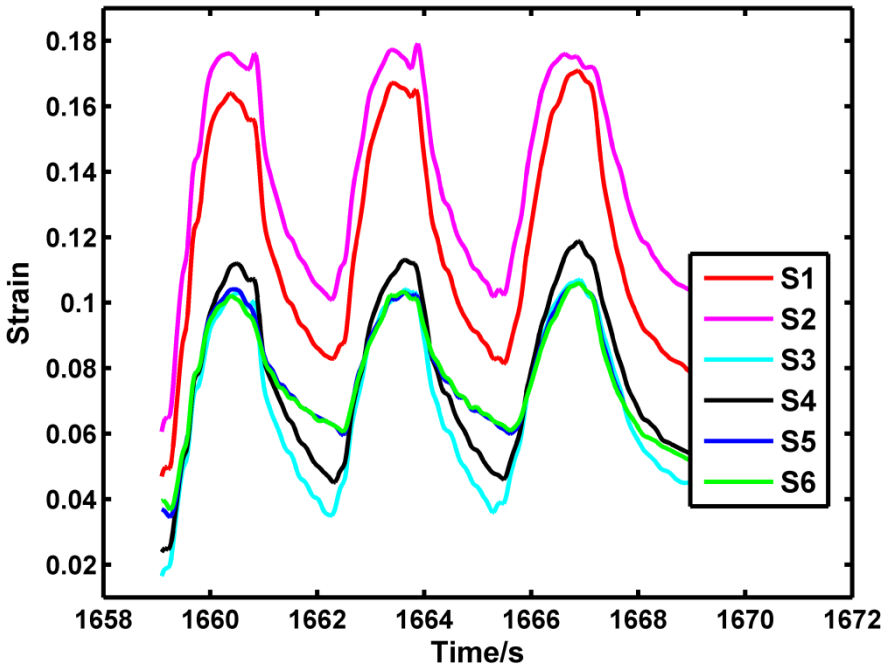

Figure 5 Similar trends of strains measured by FSSs in different positions

The sensing belts of various sizes were fabricated for different size of human upper arms. Since a maximum contact pressure of 4.3kPa/50mmHg [40] on human skin is commonly accepted and considered by many researchers and clinicians to be the safety limit to avoid ulcer due to micro-circulation damage, the size of belt should suit for different size of human

limb. A simple cylinder model of human limb is adopted to estimate the pressure exerted on human skin. Preliminary tests indicated that for ordinary people, the circumferential strain of the subjects' upper arm would not excess a maximum value of 25%. According to the cylinder model, the relation between pressure and strain of the belt is as below

$$P = \frac{2\pi}{bl} \cdot F = \frac{2\pi}{b} \cdot k \cdot 25\% < 4.3\,\text{kPa} \tag{2}$$

Where P is the pressure exerted on human skin, F is the tension in the belt, b is the breadth of the belt, l is the original length of the belt, k (Unit: N) is the stiffness of the sensing belt.

Most ordinary sizes of the limbs in the upper arm were considered, and the belts were selected accordingly (table 3).

Table 3 Designed belt size for different sizes of human upper arms

Size of sensing belts	Designed size (cm)	Suitable for upper arm size (cm)
XS	24	25 - 27
S	26	27 - 31
M	29.5	31 - 34
L	32	34 - 37

2.4. Data acquisition module and data processing

A data acquisition/transmission module via Bluetooth for LMS (Figure 2(a) has been developed. Through the '$n+1$' array, voltage signals on the FSSs were extracted from voltage dividers (Rref = 30 kΩ, 3.3 V supply by the Li-ion battery) and sent to the embedded analog-to-digital (A/D) converter. Real-time resistances of FSSs were then calculated through

digital voltage and transferred to PC via Bluetooth antenna.

$$V_s = \frac{R_{ref}}{R_{ref} + R_s} V_0$$
$$R_s = R_{ref} \cdot \left(\frac{V_0 - V_s}{V_s} \right) \tag{3}$$

where V_s is the voltage of the FSS, V_0 is supplying voltage, R_{ref} is the resistance for reference and R_s is the resistance of the FSS. The DAQ module with a small size (1.5cm×3.5cm×4.5cm) and light weight (about 30g), was packaged tightly to be wearable for daily use or sports training purpose. The sampling frequency of the LMS was set to 32Hz in this work, which is adequate to capture muscle deformation during motion, and its rechargeable battery (integrated in DAQ) can serve for 2 hours, which is sufficient for most training uses.

Resistance of FSSs in the sensing belt were captured and transferred by DAQ to user interface on remote PC and processed to obtain current strains of FSSs. Figure 3(b) reveals the linear electrical-mechanical properties of the FSSs within their effective measuring range. Once the slope of resistance ratio over strain is obtained from the LMS calibration, strain of FSSs can be measured from their resistance rate:

$$\frac{R_s - R_0}{R_0} = K \cdot \varepsilon_s \tag{4}$$

where R_s is the resistance of the FSS at current strain ε_s, R_0 is its initial resistance and K is the slope obtained from calibration of the LMS.

The limb's circumference can be calculated using the strains measured by the FSSs in the

sensing belt, whose overall length consists of length of the FSSs and the gaps between them (Figure 4). Circumference of the sensing belt (LC) can be calculated as:

$$LC = \sum_{1\le i\le N} L_{si}\cdot\left(1+s_{i0}+s_i\right)+\sum_{1\le j<N} c_j\cdot\left(1+\alpha\cdot\frac{s_j+s_{j+1}}{2}\right)+c_N\cdot\left(1+\alpha\cdot\frac{s_n+s_1}{2}\right) \tag{5}$$

where, L_{si} is the origin length of the i th FSS, s_i is the strain measured by i th FSS and s_{i0} is the pre-stretching strain of i th FSS and c_j is the gap between two adjacent FSSs.

The formula above is based on the assumption that tension of the gap c_i is approximated by the average of the tensions at its two ends:

$$\begin{aligned}&\left(k_s+k_c\right)\frac{1}{2}\left(s_j+s_{j+1}\right)\cdot\left(L_{s_j}+L_{s_{j+1}}\right)=k_c\cdot\varepsilon_{c_j}\cdot c_j\\&\varepsilon_{c_j}\approx\frac{\left(k_s+k_c\right)\cdot\bar{L}_{s_j}}{k_c\cdot c_j}\cdot\frac{1}{2}\left(s_j+s_{j+1}\right)=\alpha\cdot\frac{s_j+s_{j+1}}{2}\end{aligned} \tag{6}$$

where k_s and k_c are the stiffness of the FSS and carrier, respectively. ε_{c_j} denotes the strain of the $j\,th$ gap between $j\,th$ sensor and $j+1th$ sensor, and $\bar{L}_{s_j}$ is the average sensors' length around the sensing belt, i.e..

$$\bar{L}_{s_j}=\frac{1}{N}\sum_{1}^{N}L_{si} \tag{7}$$

The above formula has already taken into consideration that the stiffness of the belt is not uniform along the length direction. The FSSs increased the stiffness of the belt and made the sections containing FSSs stiffer than the gaps. The obtained circumference is finally transferred to circumferential ratio, the LCS, which is apparent the strain of LC.

2.5. Calibration

Before been mounted on subjects for tests, sensing belt of the LMS was calibrated with a lab-made device (Figure 6). Fixed on the shafts, the sensing belt was stretched firstly to 5% strain and then 15% strain to obtain the strain sensitivity of each FSS. Only then can the in-position strains be measured and the LC and LCS are calculated.

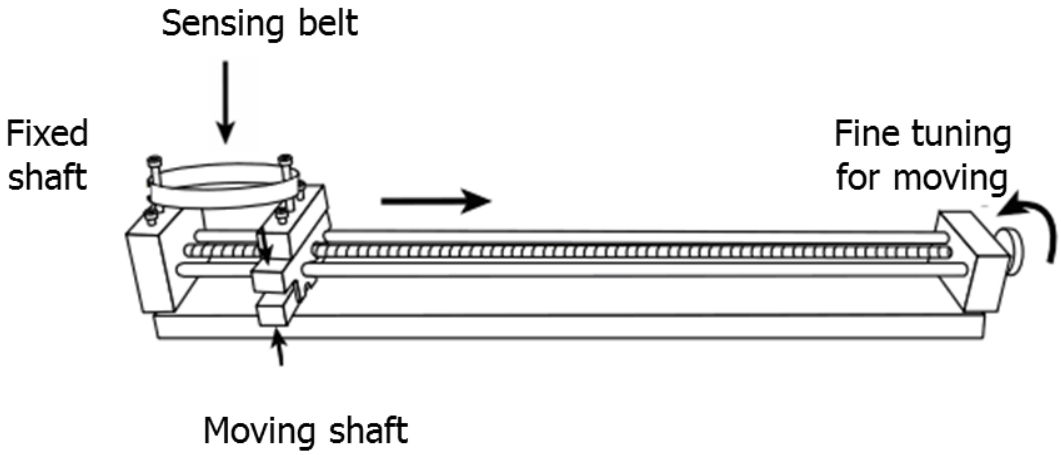

Figure 6 Calibration device

2.6. System features of LMS

The LMSs designed for the human upper arm cover a size range from 25cm to 37cm, sufficient for a wide variety of ordinary people. After calibration, cyclic test (5%~30% strain) and relaxation test was conducted with INSTRON® 5944 for the LMS of XS size (designed size 24cm), revealing a measuring accuracy of ±5% and a zero drift of about 3% within 12min. Figure 7(a) shows typical correlation between measured stain and real strain, with a good linearity of 998‰. Figure 7(b) and (c) illustrates the real strain applied by INSTRON and measured strain by LMS during cyclic loading-unloading test, respectively.

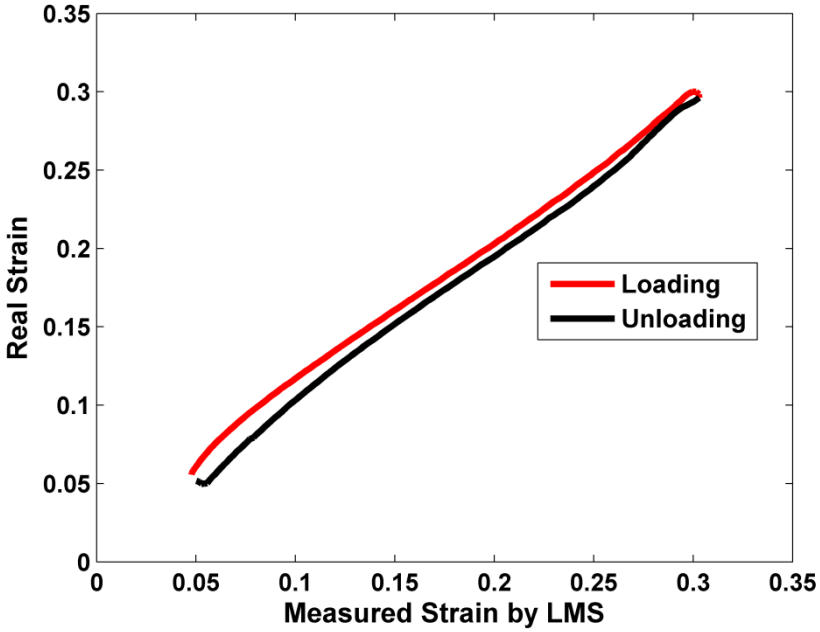
Real Strain
Measured Strain by LMS
Loading
Unloading
0.35
0.3
0.25
0.2
0.15
0.1
0.05
0
0
0.05
0.1
0.15
0.2
0.25
0.3
0.35

(a)

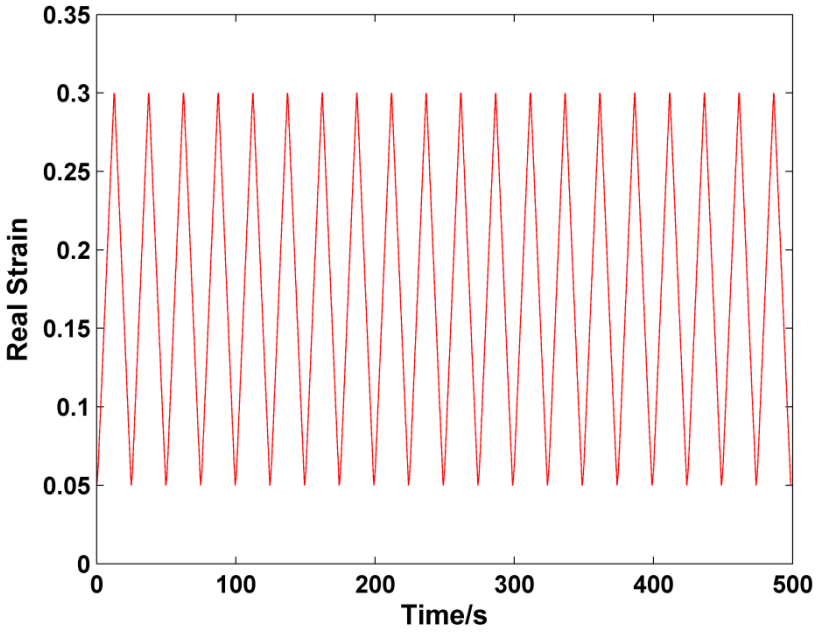
Real Strain
Time/s
0.35
0.3
0.25
0.2
0.15
0.1
0.05
0
0
100
200
300
400
500

(b)

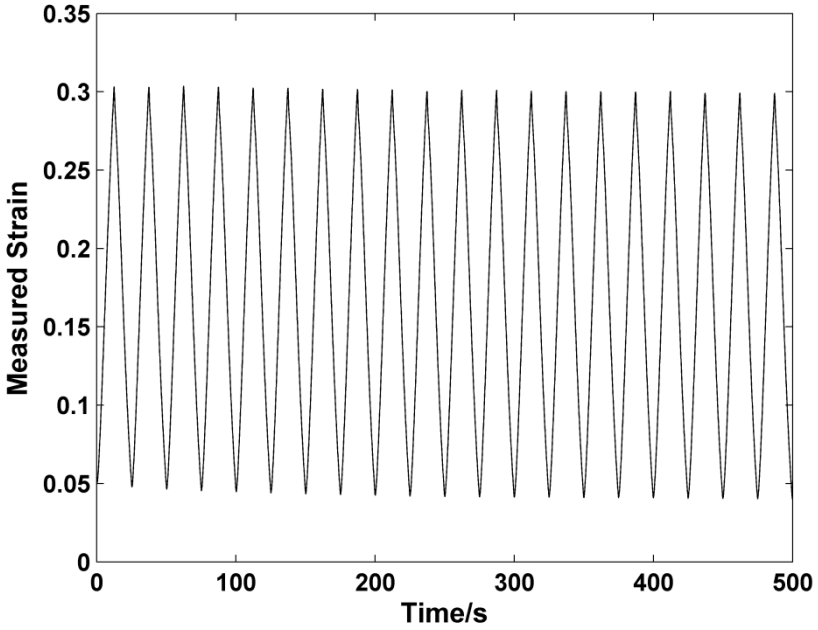

(c)

Figure 7 (a) Typical curve of measured strain-real strain of LGMS, (b) Real strain to time during cyclic loading-unloading test, (c) Measured strain to time during loading-unloading test.

Resistance relaxation causes errors for conductive materials under applied tension or compression. In the relaxation test, in which the sensing belt was stretched and held at 20%, an error due to relaxation of 8% strain was observed in the first 5 seconds, as long as one attempt in the isometric test could take at most. However, since the holding and relaxing phase of skeletal muscles was difficult to study [23], most of previous works were based on the loading phase of skeletal muscles instead of relaxation phase [6, 9, 15, 16, 34]. Hence in the current research, only the loading phase was analyzed.

3. Experimental

3.1 Subjects and setup

10 healthy right-handed male subjects participated in this study, including 2 professional

canoeists and 8 ordinary healthy persons, aged from 15 to 32 years old, with height between 164 and 175cm and weighted between 62 and 79kg. The institutional research ethics committee reviewed and approved this research. All subjects signed the informed consent form before participation. Of all the 10 subjects, LMS data of subject 1 to 8 will be analyzed in this research. The 2 professional canoeists took part in an experiment where the comparison between EMG and the LMS was made. Before the experiments, consents on data privacy and testing risks were obtained. Physical characteristics of the subjects were summarized in table 4.

Table 4 Physical characteristics of subjects

Subjects No. (ordinary persons)	Age (Years old)	Gender	Height (cm)	Weight (kg)	BMI	Dominant Hand	Upper arm Circum. (extended and relaxed) (cm)
1	29	M	175.0	72.5	23.7	R	27.5
2	31	M	164.0	68.0	25.3	R	28.0
3	31	M	175.0	70.0	22.9	R	29.2
4	29	M	175.0	79.5	26.0	R	33.0
5	24	M	164.0	63.0	23.4	R	30.0
6	25	M	174.5	64.5	21.1	R	28.0
7	35	M	175.5	72.0	23.3	R	29.0
8	32	M	174.6	66.1	21.7	R	29.5

After the calibration, the sensing belt was mounted on the location of the maximum circumference of one subject's upper arm with flexed elbow at 120°, as shown in Figure 8(a). The subject was seated and firmly fixed on Biodex machine (Biodex isokinetic testing system 3, New York, USA), which measured and recorded the elbow position and the generated torque of the elbow. Subject's right elbow was placed on a fulcrum appropriately to make axis of the elbow overlap the axis of the lever arm, so that flexion and extension of the elbow could be freely made. Elbow attachment of the elbow was adjusted properly so that the

subject's elbow could flex in a plane parallel to the one that the level arm swept in. The Biodex system was prepared and set to isometric mode. Normalized torque (NT) -time curves were obtained for each subject.

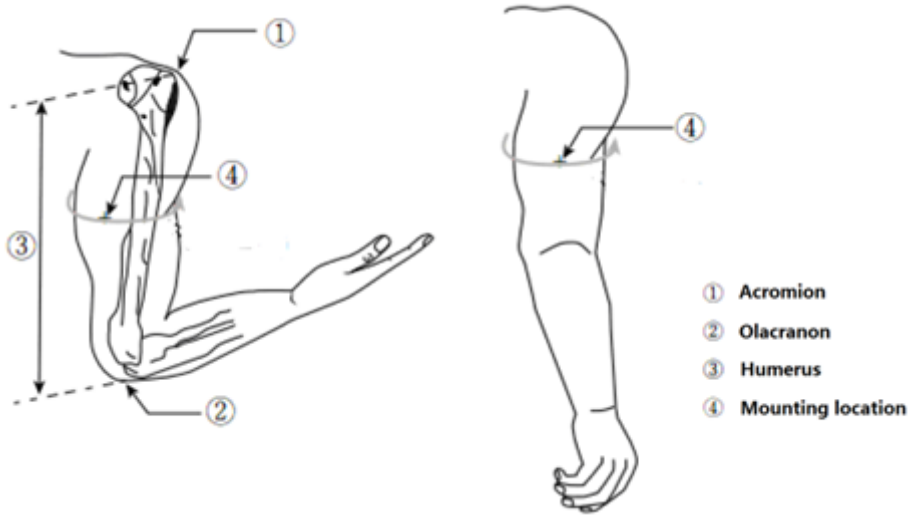

(a)

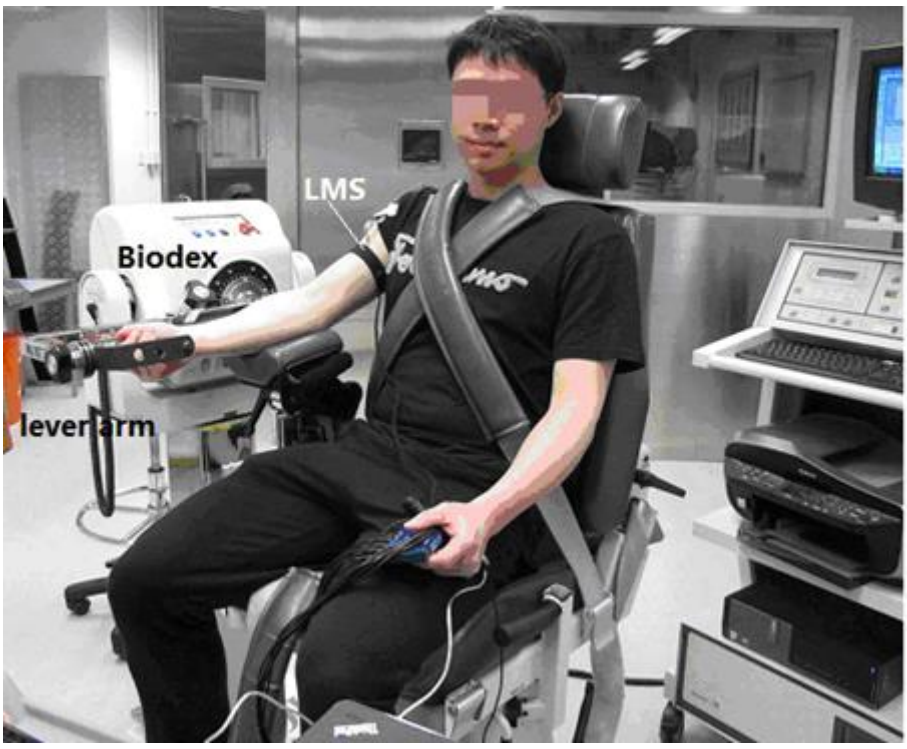

(b)

Figure 8 (a) Mounting location of the sensing belt on subject's upper arm, (b) Experimental setup

An impulse circuit generated an impulse as a synchronization signal and sent it to two laptops.

One was connected to Biodex, which recorded the elbow position and torque signals at a sampling rate of 1500Hz; the other functioned as a receiver of the LMS via Bluetooth, sampling rate of which was set to 32Hz. The two sets of data, that is, the torque values from Biodex and circumference values from the LMS were compared and correlated. Setup of the experiment is shown in Figure 8(b), in which the elbow position was fixed at 30º.

3.2. Testing protocol: Isometric contraction test

The generated torque ($= F \cdot m$, m is the moment arm of biceps to the elbow joint) has been a commonly used representation of contractile force of the skeletal muscles such as biceps in upper arm and quadriceps in thigh [7, 15, 16, 34], especially for isometric contraction mode, in which joint position keeps unchanged and the moment arm (m) of the skeletal muscles to the joint keeps constant during movement.

The level arm of Biodex was fixed to different positions, 30º, 60º, 75º, 90º and 120º, respectively. For each action, the subject was encouraged to perform a maximum voluntary isometric contraction (MVC, the maximal measured value of torque) against the fixed level arm, hold on for 2 seconds and then relaxed. Each action was followed by a 1-min rest to avoid muscle fatigue. Two trials were taken for each position. Real-time torque was shown on the screen of Biodex, and real-time circumference was displayed on program interface of the LMS on PC.

4. Data Analysis

Real-time torque is normalized by MVC of the same subject during all the isometric tests, which yields NT, while LCS is as defined in Equation 1. The typical raw data of the real-time NT and real-time LCS are plotted in Figure 9(a).

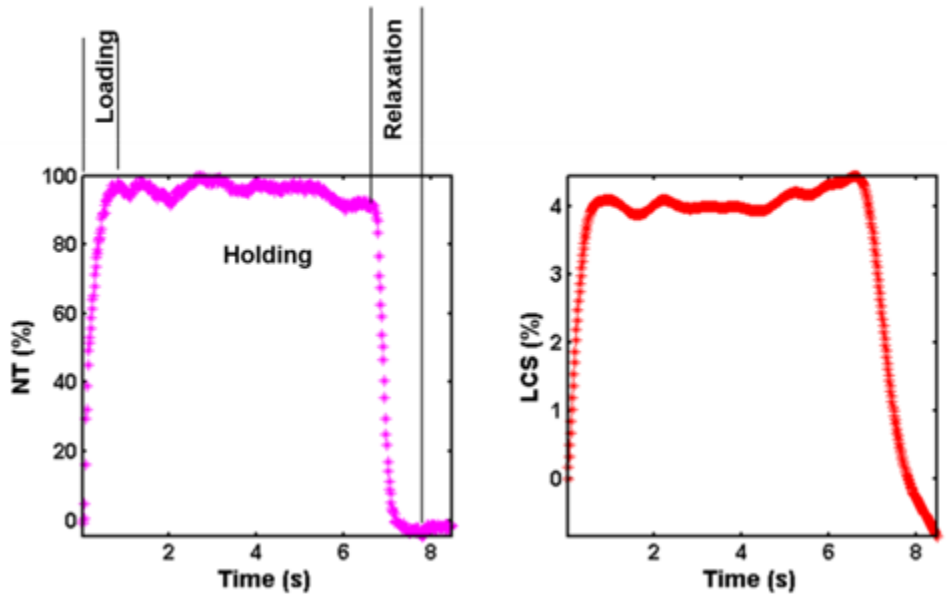

(a)

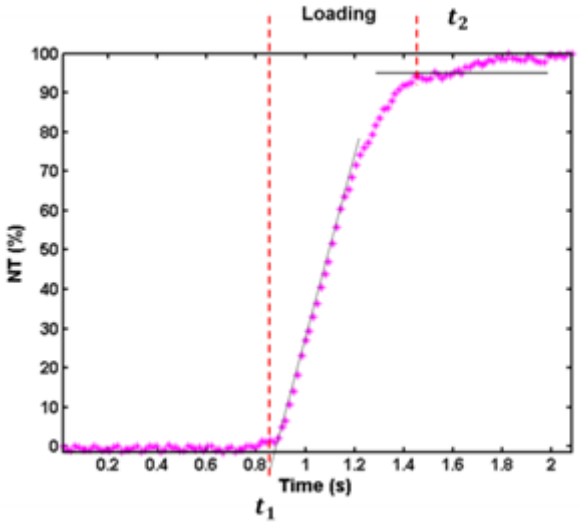

(b)

Figure 9 (a) Typical normalized torque (NT) and limb circumferential strain (LCS) during isometric test, (b)Definition of loading phase ($t_1 - t_2$)

During the isometric contractions, torque generated by biceps went through loading phase,

holding phase and relaxation phase, in sequence. Since it was much more complex to analyze skeletal muscles' performance during relaxation [23], and holding phase could not reflect dynamic change of circumference or torque, attention was only paid to the loading phase, which is defined in Figure 9(b).

Linear regression between the NT and LCS was performed for each trial and for each subject. Two dominant target parameters were studied, i.e., the proportional ratio and the linearity of the regression between the NT and LCS. The normalized torque and LCS during the loading phase of isometric mode and the proportional coefficient (α) of NT to LCS are calculated as below:

$$\begin{aligned} NT &= \frac{T}{\max(T)}; \\ \alpha &= \frac{NT}{LCS} \end{aligned} \tag{8}$$

where T is the generated torque, LCS is the limb circumferential strain, as defined in (1) , α is the ratio between NT and LCS.

In order to evaluate the result of the regression between parameters, the correlation coefficient is calculated from the following formula:

$$R = \frac{conv(X,Y)}{\sigma(X)\cdot\sigma(Y)} \tag{9}$$

where $conv$ is the operator of convolution, X and Y denote two different discrete time-variant sources of data collected, respectively.

Torque and upper arm circumference were conducted simultaneously on subjects, to verify the relation between LCS and NT. Curve fittings were performed using the following linear forms:

$$NT = \alpha \cdot LCS + \beta \tag{10}$$

The fitting coefficients α, β are determined by the least square method. α is the proportional ratio of NT to LCS and β denotes the fitting error. For the 8 subjects in isometric contraction, correlations were calculated as aforementioned. LCS and the NT are curve-fitted using the linear function as above.

5. Results and Discussions

5.1 Results

Ratio of the NT over LCS (α) and the correlation coefficient (R) with regard to subjects and positions are summarized (see table 5 and table 6, proportional ratio of NT/LCR (α) and correlation coefficients (R) of NT and LCS for every Isometric MVC of subject 1-8) and shown in Figure 10(a) and (b) respectively.

Table 5 Ratio of NT/LCR (α) for every Isometric MVC of subject 1-8

Subject No. / Position	1	2	3	4	5	6	7	8
0°	64.32	14.30	223.78	35.10	9.74	18.70	21.95	33.96
0°	61.56	24.91	281.04	14.84	11.39	7.18	19.55	17.33
30°	27.55	15.49	31.10	24.36	16.53	21.05	15.62	8.96
30°	34.95	29.83	31.03	51.95	18.12	11.50	16.76	13.97
45°	27.19	29.98	39.44	15.42	11.96	7.29	11.58	11.94
45°	28.92	33.84	86.80	21.50	14.04	7.47	9.39	14.21

60°	24.17	45.09	67.00	27.22	9.05	5.21	9.65	11.63
60°	21.77	29.98	13.07	21.88	10.18	12.87	8.32	9.66
90°	7.96	28.52	7.95	27.26	8.33	7.18	8.05	9.69
90°	8.90	16.83	6.44	25.50	9.62	9.93	10.65	12.78

Table 6 Correlation coefficients of NT & LCR in isometric maximum voluntary contraction of subject 1-8

Subject No. / Position	1	2	3	4	5	6	7	8
0	0.9450	0.9164	0.9645	0.9071	0.7088	0.9852	0.8988	0.8878
0	0.9804	0.9881	0.6883	0.9868	0.8438	0.9098	0.8202	0.9424
30	0.9816	0.7855	0.9468	0.9773	0.8034	0.9249	0.8842	0.9731
30	0.9625	0.9955	0.9625	0.8272	0.9486	0.9532	0.9002	0.9783
45	0.9566	0.9857	0.9811	0.9902	0.9810	0.8422	0.9314	0.9682
45	0.9739	0.9756	0.9900	0.9625	0.9781	0.8861	0.8830	0.9870
60	0.9749	0.9705	0.9769	0.9646	0.9068	0.9584	0.9129	0.9633
60	0.9782	0.9775	0.9733	0.9929	0.9708	0.7234	0.9162	0.9740
90	0.9655	0.9804	0.9727	0.9810	0.9598	0.9296	0.9374	0.9354
90	0.9356	0.8854	0.9534	0.8955	0.9698	0.9756	0.9686	0.8804

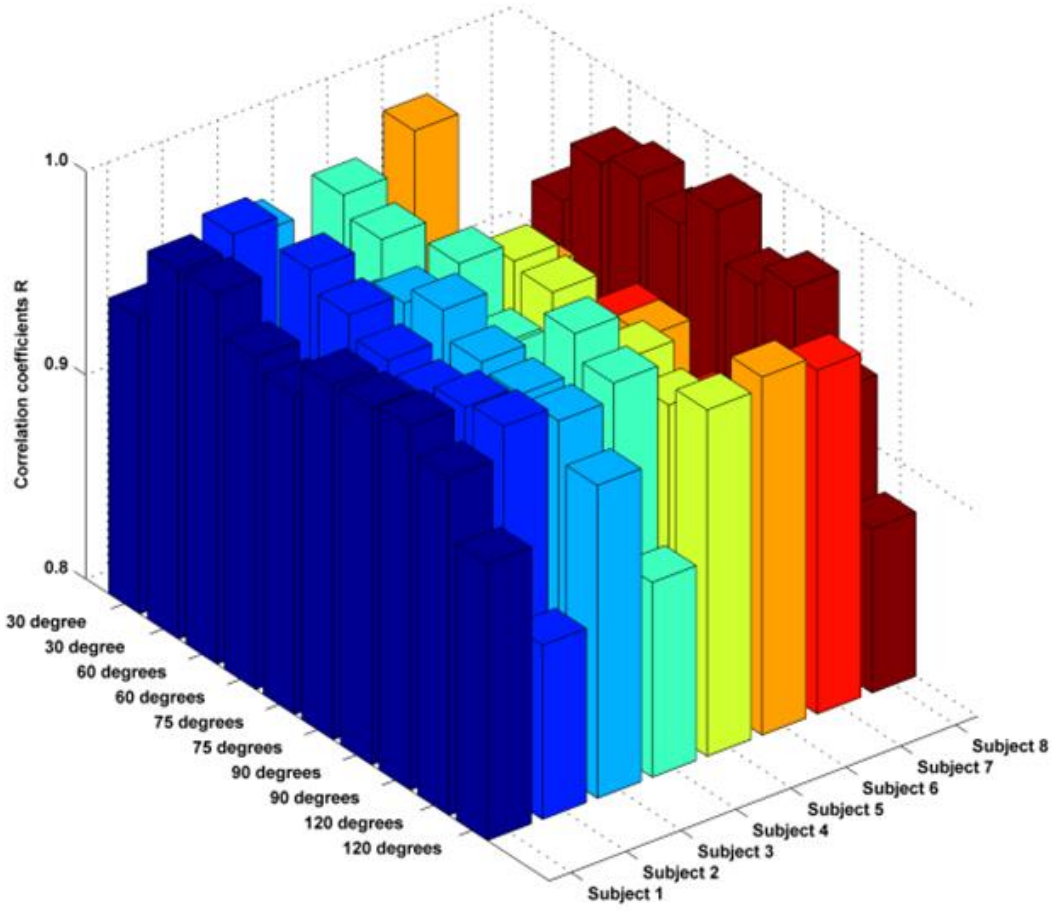
Correlation coefficients R
1.0
0.9
0.8
30 degree
30 degree
60 degrees
60 degrees
75 degrees
75 degrees
90 degrees
90 degrees
120 degrees
120 degrees
Subject 1
Subject 2
Subject 3
Subject 4
Subject 5
Subject 6
Subject 7
Subject 8

(a)

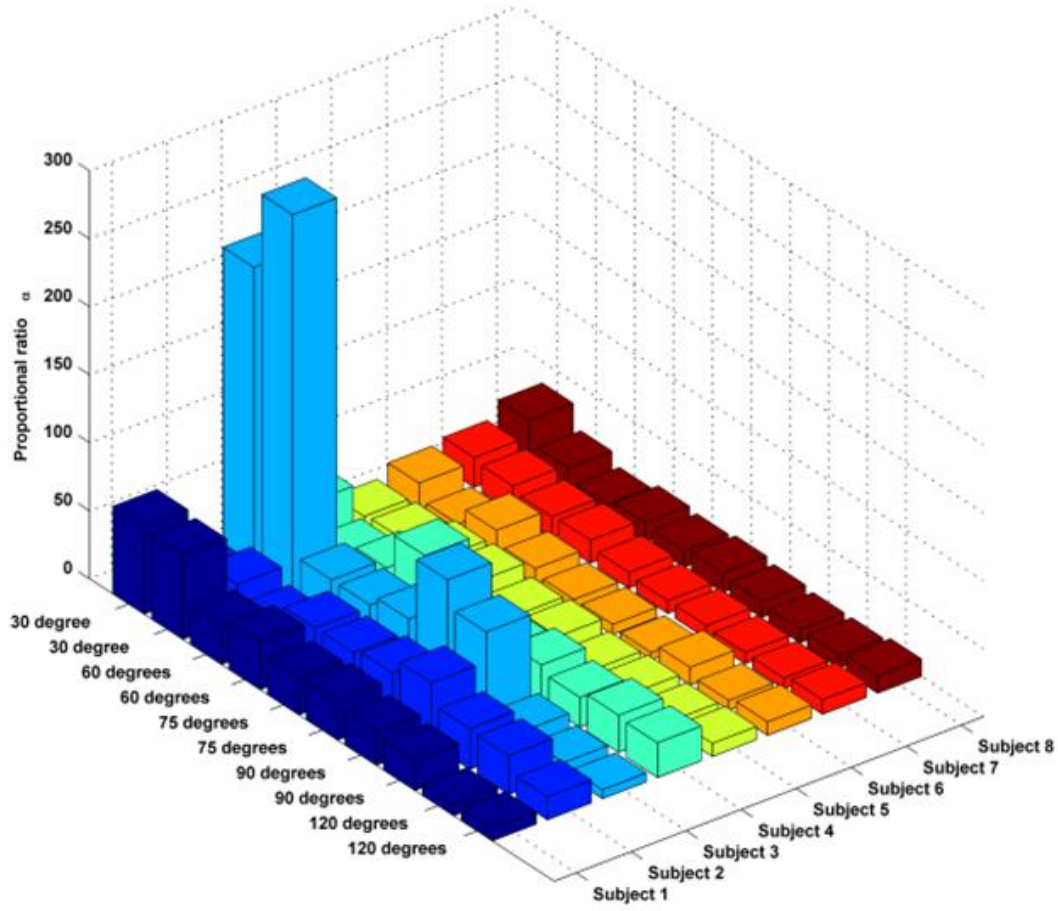

(b)

Figure 10 (a) Ratio of NT/LCS (α) for every Isometric MVC of subjects 1 to 8, (b) Correlation coefficients of NT & LCS in Isometric MVC of subjects 1 to 8

Proportional coefficient of NT to LCS (coefficient α), which stand for the sensitivity of contractile force of biceps brachii to the upper arm's circumferential strain (LCS), was summarized in table 7 for the eight subjects, as well as the correlation coefficients of LCS vs. the NT of the eight subjects (1 to 8). The correlation coefficients R are observed generally good, showing a good linear relationship between NT and LCS. The mean correlation coefficient of the trials is 0.938±0.050 (Mean±Std). Meanwhile 79% of the trials show

correlations higher than 0.9 and 51% of the trials endure correlations higher than 0.96. Two-factor ANOVA (analysis of variance) was performed on the correlation coefficients to derive the effect of the elbow positions and subjects. The results suggest that there is no significant difference between positions ($p = 0.258$) as well as subjects ($p = 0.389$), which implies that the linear relationship between the NT and LCS is generally held.

The average proportional ratios α between the NT and LCS for the 8 subjects were listed in table 7, ranging from 10.90 to 30.73. Two-factor ANOVA calculation indicates that there is no significant difference among the subjects ($p = 0.136$), however, the individual difference is significant among the total five elbow positions ($p = 0.0005$). The effect sizes for both the difference among subjects and difference among joint positions are 0.13 and 0.28, respectively, both are deemed large according to Cohen[41]. In other words, the sensitivity of NT to LCS during isometric contraction is strongly affected by positions.

Table 7 Summary of fitting coefficients (proportional ratio α and fitting error β) and the correlation coefficients (R)

Subject No. / Fitting Coe.		1	2	3	4	5	6	7	8	Avg.
α	Mean	30.73	26.88	35.35	26.50	11.90	10.84	13.15	14.41	\
	Std	18.98	9.45	28.75	10.71	3.31	5.31	4.97	7.32	
β (%)	Mean	-3.99	5.24	6.42	9.96	11.11	17.20	18.38	1.57	
	Std	9.39	10.89	9.35	9.95	10.05	13.72	5.01	13.09	
R	Mean	0.964	0.946	0.970	0.949	0.907	0.909	0.905	0.949	0.938
	Std	0.016	0.067	0.014	0.055	0.093	0.078	0.040	0.038	0.050

Table 8 Physical information of subject 9 and 10

Subjects	Age (Years old)	Gender	Height (cm)	Weight (kg)	BMI	Dominant Hand	Upper arm Circum. (extended and relaxed) (cm)
1. canoeist	15	M	170.2	63.4	21.9	R	28.0
2. canoeist	17	M	173.4	62.5	20.8	R	28.5

The feasibility of monitoring muscle contraction using LCS was indicated and further tested with 2 canoeists (see table 8, physical information of subject 9 and 10) on elbow isometric contractions. Besides torque and real-time LCS, surface electromyography (sEMG) was also measured simultaneously. Previous work [7, 16] have observed exponential relationships between normalized sEMG RMS and torque as well as between sEMG RMS and muscle deformation. Hence, the curve fittings of sEMG and were performed using the following forms:

$$\begin{aligned} LCS &= a\left(1-e^{-b\cdot E_r}\right) \\ NT &= \alpha\cdot LCS+\beta \\ NT &= g\left(1-e^{-h\cdot E_r}\right) \end{aligned} \tag{11}$$

where NT is the normalized torque, E_r is normalized EMG RMS. Typical correlations among those 3 sources of signals are shown in Figure 11. The coefficients results, a, b, α, β, g and h are determined by the least square method, and are summarized in table 9.

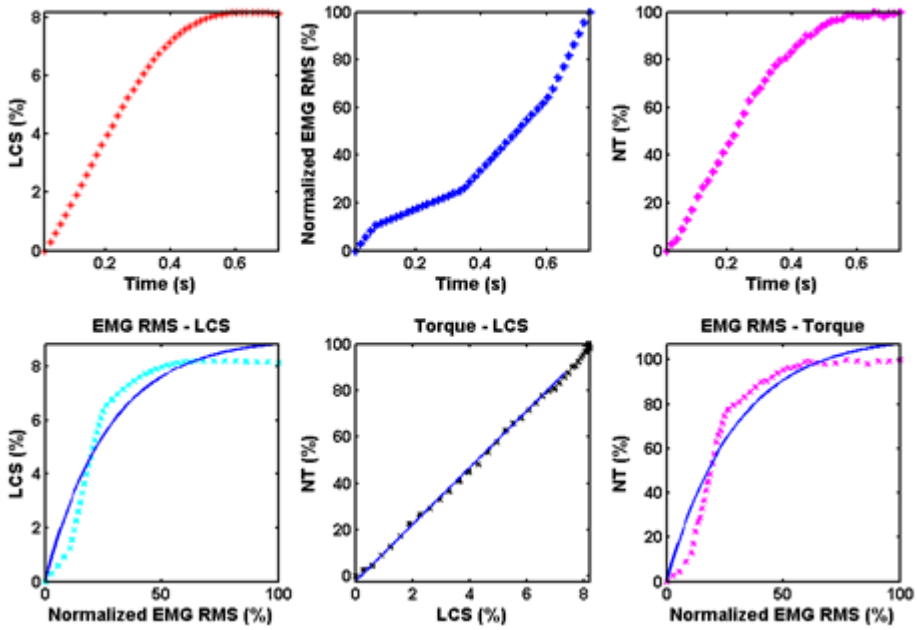

Figure 11 Typical relationships among normalized sEMG RMS, normalized torque and LCS (blue solid lines are the fitted curves)

Table 9 Coefficients of regression among sEMG RMS, NT and LCS during isometric contraction at 30º flexion

Coefficients obtained through fitting	Subject9	Subject 10	Mean ±Std
Exponential coefficient between E_r and LCS (b) ($\times 10^{-2}$)	1.45 ±1.36	2.14 ±1.22	1.75 ±2.58
Goodness of fitting between E_r and LCS (r^2)	0.979 ±0.025	0.97 ±0.028	0.975 ±0.053
Linear coefficient between NT and LCS (α)	25.6 ±11.6	28.2 ±16.1	26.8 ±27.7
Goodness of fitting between NT and LCS (r^2)	0.967 ±0.027	0.956 ±0.032	0.962 ±0.059
Exponential coefficient between normalized sEMG RMS and NT(h) ($\times 10^{-2}$)	2.75 ±1.9	4.91 ±1.95	3.83 ±1.92
Goodness of exponential fitting between normalized sEMG RMS and NT (r^2)	0.981 ±0.025	0.96 ±0.028	0.97 ±0.049

The exponential coefficient, b, between the normalized sEMG RMS and LCS is 1.75, with a goodness r^2 of 0.975. Comparison was made between current results and previous published works on torque, muscle thickness and sEMG RMS [7, 16], as the LCS was induced by the variation of biceps' thickness. The goodness of fitting is better than previous work (0.869±0.048), but the average exponential coefficient (1.75×10^{-2}) is smaller than previous published results (3.41×10^{-2}).

Linear coefficient between the normalized torque and LCS is 26.8±13.7, the goodness of linear fitting is 0.962. The good linear relationship between the NT and LCS also confirmed that LCS can serve as an index for contraction of muscle. This linear relationship occurred in all subjects under this study although individual subjects may have significant variation in the slopes of the curves, or proportional coefficient α.

Regressions among sEMG RMS, NT and LCS show an exponential relationship between sEMG and LCS, and the linear relationship between NT and LCS was re-confirmed. As LCS is another index for muscle deformation in thickness, these results were expected [7, 16].

The effective sample size should be pointed out to verify the validity of the results. With a power of 90%, correlation coefficient of 0.90 or higher to confirm a linear correlation, 0.80 or lower (correlated but ill-linear) to deny the linear correlation and the obtained standard deviation of 0.050, it can be derived that a minimal sample size of 5 subjects is required to

successfully recognize the linear correlation between LCS and NT. In this work, the sample size was satisfied by 10 subjects.

5.2 Discussions

As mentioned before, since the relaxing phase of skeletal muscles is difficult to predict [23], most of previous works have been focused on the loading phase of skeletal muscles instead of relaxation phase [6, 9, 15, 16, 34]. In current research, only the loading phase of isometric contraction has been analyzed up to now.

According to Equation 1, during elbow isometric contraction with a certain fixed position, the LCS of upper arm should be in a linear relationship with NT. However, the measured values of LCS and NT do not reveal a perfect linearity (0.9375±0.0499). Three possible factors might contribute. First, the deformation of other skeletal muscles (such as triceps and brachialis) did occur and contribute to the circumferences' variation during elbow flexion, but was considered small and ignored. Hence, the LCS could not fully represent the deformation of the biceps as assumed. Secondly, the small pressures (less than 33mmHg) exerted by the sensing belt might still hinder biceps' free deformation. Skeletal muscles are not rigid during contraction and can be squashed under pressure. However, to which extent could this pressure effect the LCS has not been considered in this work. Thirdly, the belt is assumed to contact firmly and intimately with human upper arm, and the slippage on the arm is ignored. Stress relaxation of fabrics may also cause error [38], even though the LMS was calibrated for each subject before each test. After long-time use, a sensing belt may not be tight as it was initially,

especially for later subject(s) with slim upper arms.

Subject 3 was observed with abnormally high proportional coefficients (223.78 and 281.04) for initial position 0°, as in Figure 10(a). Some possible reasons may jointly be addressed. If somehow the sensing belt was mounted lower than target location, the sensing belt could be loose and very small strain would be detected. Meanwhile, subject 3 was observed with thick fat in upper arm (although the BMI of subject 3 is 22.9), which could also obscure the circumferential strain measured during contraction. For 0° position in isometric contraction, the max LCS measured is 0.4% for subject 3, while for other subjects it is higher than 1.5%. The error in LCS measurement can finally lead to the over-calculation in proportional coefficients.

The fitting error β is the intercept of the NT-LCS linear fitting on the NT axis, and is affected by the initial status of each test. Torque and limb circumference were measured simultaneously, and according to the test protocol, each test should start from relaxation. However, it's difficult to hold the lever without exerting any torque on it. For an extreme example, during isometric contraction of 90° position, subject 6 held the lever tightly and the torque measured by Biodex started from 24.5 $N \cdot m$ other than from around 0 $N \cdot m$. In this case, the fitting error β was found as high as 40%.

According to Equation 10, the proportional coefficients represent to which extent the voluntary muscle (biceps brachii) deforms during contraction. Although linear relationship

was found between NT and LCS (as in Figure 10(b)), and the proportional coefficients are sensitive to positions, individual variation in proportional coefficients was observed between subjects. Correlation between maximum voluntary contractions (index for strength) has been calculated and proportional coefficients is -0.482, showing there is no correlation between them. These findings reveal the un-even proportional coefficient for different joint positions and for different subjects, implying the importance of studying the proportional coefficient for subjects in kinetic contraction modes, such as isokinetic contractions and isotonic contractions. Moreover, the detecting of joint position appears essential for an independent monitoring of contraction (currently the joint position was detected by the Biodex®).

The chosen FSSs in the LMS have similar mechanical-electrical properties. However, as viscoelasticity has been observed on the FSSs [38, 39], time-dependent creep effect of the FSSs in the LMS is inevitable, of which initial-resistance-drift is one of the consequences. In this study, LCS was utilized other than LC to represent the circumferential deformation of upper arm during contraction and the error caused by sensors' creep is automatically eliminated.

Based on the novel fabric strain sensors, the novel wearable fabric sensing system，LGMS , is gifted with the merits of lightweight, portability, comfort and suitable for not only research in lab and clinic, but also for fitting and sport training. However, the validity of indexing muscle contraction with LCS relies on successfully extracting the increments of circumference due to contraction. With the relaxation effect of FSSs, the measured LCS is inaccurate at small

values in extreme circumstances such as muscle fatigue or muscle pump due to excessive training, both should be avoided from working condition of the sensing device.

6. Conclusions

The paper describes a novel flexible and convenient limb anthropometric measuring device consisting of a series of FSSs, aiming to collect an anthropometric perimeter, that is, the upper arm circumference and its change ratio, the circumferential strain, during elbow flexion in isometric mode. During loading phase of isometric contraction, the normalized torque and limb circumference strain demonstrate a very good linear correlation. The experimental results confirm that the limb circumference is a useful index for muscle contraction of up-arm in isometric contraction.

More importantly, this work shows significant differences in normalized torque and limb circumference strain for the loading phase of isometric contraction at different positions, which implies that the ratio between torque increment and circumference increment highly depends on joint positions which may be one of the most important contributors to big error in [34]. The effects of joint positions are incorporated into our study of isokinetic contraction mode, and will be reported separately.

This work opens a door to an exploratory study of limb circumference strain as an index to monitor muscle deformation of other modes (isotonic and isokinetic) of contraction and different limbs and skeletal muscles. Additionally, the measurement system has been designed

for wearable and easy use in training so that its application for real-time measurement of muscle deformation and torque generated is feasible.

Acknowledgements:

The work has been partially supported by The Research Grants Council, National Science Foundation of China (Grant No. 525113 and N-PolyU503/12) and Innovation and Technology Commission (Grant No. ITT/011/11TT) of Hong Kong SAR Government. Wang X acknowledges a postgraduate scholarship from the Hong Kong Polytechnic University.

References:

[1] O.M. Blake, Y. Champoux, J.M. Wakeling, Muscle coordination patterns for efficient cycling, Med Sci Sports Exerc, 44(2012) 926-38.

[2] G. Wei, F. Tian, G. Tang, C. Wang, A Wavelet-Based Method to Predict Muscle Forces From Surface Electromyography Signals in Weightlifting, Journal of Bionic Engineering, 9(2012) 48-58.

[3] C. English, L. Fisher, K. Thoirs, Reliability of real-time ultrasound for measuring skeletal muscle size in human limbs in vivo: a systematic review, Clinical rehabilitation, 26(2012) 934-44.

[4] L.F. Oliveira, T.T. Matta, D.S. Alves, M.A. Garcia, T.M. Vieira, Effect of the shoulder position on the biceps brachii EMG in different dumbbell curls, Journal of Sports Science and Medicine, 8(2009) 24-9.

[5] J.L. Chestnut, D. Docherty, The Effects of 4 and 10 Repetition Maximum Weight-Training Protocols on Neuromuscular Adaptations in Untrained Men, The Journal of Strength & Conditioning Research, 13(1999) 353-9.

[6] R.M. Campy, A.J. Coelho, D.M. Pincivero, EMG-torque relationship and reliability of the medial and lateral hamstring muscles, Med Sci Sports Exerc, 41(2009) 2064-71.

[7] J. Shi, Y.P. Zheng, Q.H. Huang, X. Chen, Continuous monitoring of sonomyography, electromyography and torque generated by normal upper arm muscles during isometric contraction: Sonomyography assessment for arm muscles, Ieee T Bio-Med Eng, 55(2008) 1191-8.

[8] E.J. Jones, P.A. Bishop, A.K. Woods, F.M. Green, Cross-Sectional Area and Muscular Strength A Brief Review, Sports Med, 38(2008) 987-94.

[9] J. Davies, D.F. Parker, O.M. Rutherford, D.A. Jones, Changes In Strength And Cross-Sectional Area Of the Elbow Flexors as a Result Of Isometric Strength Training, Eur J Appl Physiol O, 57(1988) 667-70.

[10] T. Fukunaga, M. Miyatani, M. Tachi, M. Kouzaki, Y. Kawakami, H. Kanehisa, Muscle volume is a major determinant of joint torque in humans, Acta Physiol Scand, 172(2001) 249-55.

[11] R. Akagi, Y. Takai, M. Ohta, H. Kanehisa, Y. Kawakami, T. Fukunaga, Muscle volume compared to cross-sectional area is more appropriate for evaluating muscle strength in young and elderly individuals, Age Ageing, 38(2009) 564-9.

[12] S.R. Perry-Rana, T.J. Housh, G.O. Johnson, A.J. Bull, J.T. Cramer, MMG and EMG responses during 25 maximal, eccentric, isokinetic muscle actions, Med Sci Sport Exer, 35(2003) 2048-54.

[13] H.S. Milner-Brown, R.B. Stein, The relation between the surface electromyogram and muscular force, The Journal of Physiology, 246(1975) 549-69.

[14] J.H. Lawrence, C.J. De Luca, Myoelectric Signal Versus Force Relationship In Different Human Muscles, J Appl Physiol, 54(1983) 1653-9.

[15] E.A. Clancy, O. Bida, D. Rancourt, Influence of advanced electromyogram (EMG) amplitude processors on EMG-to-torque estimation during constant-posture, force-varying contractions, J Biomech, 39(2006) 2690-8.

[16] J.Y. Guo, Y.P. Zheng, H.B. Xie, X. Chen, Continuous monitoring of electromyography (EMG), mechanomyography (MMG), sonomyography (SMG) and torque output during ramp and step isometric contractions, Med Eng Phys, 32(2010) 1032-42.

[17] N. Shima, C.J. McNeil, C.L. Rice, Mechanomyographic and electromyographic responses to stimulated and voluntary contractions in the dorsiflexors of young and old men, Muscle Nerve, 35(2007) 371-8.

[18] M.V. Narici, G.S. Roi, L. Landoni, A.E. Minetti, P. Cerretelli, Changes In Force, Cross-Sectional Area And Neural Activation during Strength Training And Detraining Of the Human Quadriceps, Eur J Appl Physiol O, 59(1989) 310-9.
[19] M.O. Ibitoye, N.A. Hamzaid, J.M. Zuniga, A.K.A. Wahab, Mechanomyography and muscle function assessment: A review of current state and prospects, Clinical Biomechanics, 29(2014) 691-704.
[20] R. Akagi, S. Iwanuma, S. Hashizume, H. Kanehisa, T. Fukunaga, Y. Kawakami, Determination of Contraction-Induced Changes in Elbow Flexor Cross-Sectional Area for Evaluating Muscle Size-Strength Relationship during Contraction, Journal of Strength and Conditioning Research, 29(2015) 1741-7.
[21] D.B. Starkey, M.L. Pollock, Y. Ishida, M.A. Welsch, W.F. Brechue, J.E. Graves, et al., Effect of resistance training volume on strength and muscle thickness, Medicine and science in sports and exercise, 28(1996) 1311-20.
[22] R. Akagi, S. Iwanuma, M. Fukuoka, H. Kanehisa, T. Fukunaga, Y. Kawakami, Methodological Issues Related to Thickness-Based Muscle Size Evaluation, J Physiol Anthropol, 30(2011) 169-74.
[23] P.W. Hodges, L.H.M. Pengel, R.D. Herbert, S.C. Gandevia, Measurement of muscle contraction with ultrasound imaging, Muscle Nerve, 27(2003) 682-92.
[24] R. Akagi, Y. Takai, E. Kato, M. Fukuda, T. Wakahara, M. Ohta, et al., Relationships between Muscle Strength and Indices of Muscle Cross-Sectional Area Determined during Maximal Voluntary Contraction in Middle-Aged and Elderly Individuals, Journal of Strength and Conditioning Research, 23(2009) 1258-62.
[25] R. Akagi, H. Kanehisa, Y. Kawakami, T. Fukunaga, Establishing a new index of muscle cross-sectional area and its relationship with isometric muscle strength, Journal of Strength and Conditioning Research, 22(2008) 82-7.
[26] J.A.R. Cannan, H.S. Hu, Automatic Circumference Measurement for Aiding in the Estimation of Maximum Voluntary Contraction (MVC) in EMG Systems, Lect Notes Artif Int, 7101(2011) 202-11.
[27] L.A. Green, D.A. Gabriel, Anthropometrics and electromyography as predictors for maximal voluntary isometric arm strength, J Sport Health Sci, 1(2012) 107-13.
[28] F. Lemma, P. Shetty, Seasonal variations in the relationship between mid-upper arm circumference and maximum voluntary contraction among ethiopian farmers, Eur J Clin Nutr, 63(2009) 513-20.
[29] W. Zeng, L. Shu, Q. Li, S. Chen, F. Wang, X.M. Tao, Fiber-based wearable electronics: a review of materials, fabrication, devices, and applications, Advanced materials, 26(2014) 5310-36.
[30] L. Cai, L. Song, P. Luan, Q. Zhang, N. Zhang, Q. Gao, et al., Super-stretchable, transparent carbon nanotube-based capacitive strain sensors for human motion detection, Scientific reports, 3(2013) 3048.
[31] D. Son, J. Lee, S. Qiao, R. Ghaffari, J. Kim, J.E. Lee, et al., Multifunctional wearable devices for diagnosis and therapy of movement disorders, Nature nanotechnology, 9(2014) 397-404.
[32] D.I. Kim, T. Quang Trung, B.U. Hwang, J.S. Kim, S. Jeon, J. Bae, et al., A Sensor Array Using Multi-functional Field-effect Transistors with Ultrahigh Sensitivity and Precision for Bio-monitoring, Scientific reports, 5(2015) 12705.
[33] D.Q. Ying, X.M. Tao, W. Zheng, G.F. Wang, Fabric strain sensor integrated with looped polymeric optical fiber with large angled V-shaped notches, Smart Materials and Structures, 22(2013).
[34] W.S. Kim, H.D. Lee, D.H. Lim, J.S. Han, K.S. Shin, C.S. Han, Development of a muscle circumference sensor to estimate torque of the human elbow joint, Sensors and Actuators A: Physical, 208(2014) 95-103.

[35] G. Pollack, Contractile mechanisms in muscle: Springer Science & Business Media; 2013.
[36] F. Wang, B. Zhu, L. Shu, X.M. Tao, Flexible pressure sensors for smart protective clothing against impact loading, Smart Materials and Structures, 23(2014).
[37] L. Shu, T. Hua, Y.Y. Wang, Q.A. Li, D.D. Feng, X.M. Tao, In-Shoe Plantar Pressure Measurement and Analysis System Based on Fabric Pressure Sensing Array, Ieee T Inf Technol B, 14(2010) 767-75.
[38] Y.Y. Wang, T. Hua, B. Zhu, Q. Li, W.J. Yi, X.M. Tao, Novel fabric pressure sensors: design, fabrication, and characterization, Smart Mater Struct, 20(2011).
[39] W.J. Yi, Y.Y. Wang, G.F. Wang, X.M. Tao, Investigation of carbon black/silicone elastomer/dimethylsilicone oil composites for flexible strain sensors, Polymer Testing, 31(2012) 677-84.
[40] M. Kalani, K. Brismar, B. Fagrell, J. Ostergren, G. Jorneskog, Transcutaneous oxygen tension and toe blood pressure as predictors for outcome of diabetic foot ulcers, Diabetes Care, 22(1999) 147-51.
[41] J. Cohen, Statistical power analysis for the behavioral sciences (revised ed.), New York: Academic Press1977.